Synthesis, Thermal Degradation, and Flame Retardance of Novel Triazine Ring-Containing Macromolecules for Intumescent Flame Retardant Polypropylene

Jinfeng Dai, Bin Li

Heilongjiang Key Laboratory of Molecular Design and Preparation of Flame Retarded Materials, College of Science, Northeast Forestry University, Harbin 150040, People's Republic of China

ABSTRACT: Two novel triazine ring-containing macromolecules, designated as charring-foaming agent 1 (CFA1) and charring-foaming agent 2 (CFA2), were synthesized by a series of polycondensation reactions. Their chemical structures were analyzed by Fourier transform infrared spectroscopy (FTIR), nuclear magnetic resonance spectroscopy (^{13}C solid-state NMR), and elemental analysis, and their thermal degradation properties were assessed by thermogravimetric analysis (TGA). TGA data revealed that CFA1 and CFA2 show high thermal stability and have a high propensity for char formation, their initial decomposition temperatures being 300.2°C and 287.1°C, and their char residues at 800°C amounting to 32.2 wt % and 21.1 wt %, respectively. CFA1 presents higher thermal stability and more char residue than CFA2. Based on experimental results of the flame retardancy (limiting oxygen indices values and UL-94 V-0 rating) and the TG data of new intumescent flame retardant polypropylene (IFR-PP) containing CFA1 and CFA2, CFA1 exhibits more outstanding intumescent flame retardance than CFA2. IFRs containing CFA1 and CFA2 enhanced Notched Izod Impact strength of IFR-PP, and slightly lower tensile strength of IFR-PP. IFR2 shows more advantageous effect on mechanical properties of IFR-PP than IFR1. © 2010 Wiley Periodicals, Inc. J Appl Polym Sci 116: 2157–2165, 2010

Key words: triazine ring-containing macromolecule; synthesis; thermal degradation; flame retardance; polypropylene

INTRODUCTION

The great proliferation in the use of polymeric materials that has occurred in the last few decades has led to an increase of fire risks. In particular, the use of polyolefins in electric and electronic, building, or transport aspects is strongly limited because of their easy flammability with low limiting oxygen indices (LOI), which are of the order of 17.5%[1]. Accordingly, flame-retardant polyolefins are urgently needed.

As is well-known, the most effective flame retardants for polyolefins are halogen-based flame retardants.[2] However, the use of these flame retardants is restricted owing to the extensive release of toxic and corrosive fumes during their decomposition,[3] which would result in ecological and physical problems. Metal hydroxides are another class of flame-retardant additives used in polyolefins,[4–6] but high loadings of these are seriously detrimental to the mechanical properties of polymeric materials. Therefore, intumescent flame retardants (IFRs) are a growing group of halogen-free agents that are at the forefront of interest concerning environmentally friendly flame retardants due to their advantages of little smoke and low toxicity during burning.[3,7–20] In particular, they have shown good efficiency in the flame retardation of polyolefins.

A typical IFR mainly comprises three basic elements, namely, an acid source, a char-forming agent, and a blowing agent. Such a system can undergo an intense expansion and form a protective foamed char layer, thus effectively holding back the transfer of the heat and fuel during combustion and resulting in quick self-extinguishing of the burning material.[21–25] However, most existing IFRs have some deficiencies, such as lower flame-retardant efficiency, lower thermal stability, lower water resistance, and poor compatibility, although several approaches[26] have been studied for improving IFR systems. Consequently, the challenge for further investigations lies in the preparation of new IFRs with high char residues, high thermal stability, good processing properties, and high flame retardance.

In recent years, nonconjugated polymers and supramolecular structures containing 1,3,5-triazine

rings have received much attention in industry because of their high thermal stability derived from the structural symmetry of the 1,3,5-triazine ring.[27–31] Moreover, it has already been reported[32–40] that triazine-based polymers show very good flame-retardant behavior by virtue of their excellent charring effect in IFRs, which can be mainly attributed to the presence of the tertiary nitrogen in the triazine ring structure. However, because of lower thermal stability and lower char formation of some other triazine polymers,[32,33] they are not suitable for use as charring agents in IFR systems.

Therefore, based on our previous work,[37–40] in the work described that, two novel triazine-containing macromolecules have been designed and synthesized by polycondensation reactions. The triazine-containing macromolecules display high thermal stability and excellent flame retardance, which make them be suitable for application as flame retardants in most conventional polymers. The structures of the triazine-containing macromolecules have been characterized by FTIR, ^{13}C solid-state NMR, and elemental analysis. Their flammability properties and thermal degradation behavior of IFR-PP systems have been investigated by LOI, vertical burning test (UL-94), and thermogravimetric analysis (TGA).

EXPERIMENTAL

Materials

Cyanuric chloride (industrial) was purchased from the Yingkou Sanzheng Organic Chemical Industry Company, ethanolamine (analytical) and ethylenediamine (analytical) from the Tianda Chemical Reagent Factory, and 1,2-diamino-4-methylcyclopentane(DMCP, industrial) from Henan Tzarindustria Company. Piperazine (analytical) was obtained from the Sinopharm Chemical Reagent Company.

Polypropylene (PP) resin (homopolymer, melt flow rate: 3.5 g/10 min) was produced by Daqing Huake Co., China. Ammonium polyphosphate (APP, GD-101, crystalline form II, $n > 1500$, average particle size: 15 μm) was supplied by Zhejiang Longyou GD Chemical Industry Company.

Synthesis of the triazine-containing macromolecules

The two novel triazine-containing macromolecules, which are designated as charring-foaming agent 1 (CFA1) (Scheme 1) and charring-foaming agent 2 (CFA2) (Scheme 2), were synthesized according to a three-step procedure.

In the first step, cyanuric chloride (184.5 g, 1 mol) was dispersed in a mixture of acetone (500 mL) in a thoroughly dried, four-necked 2 L flask equipped with an overhead mechanical stirrer, a thermometer, a reflux condenser, and a dropping funnel. The flask was immersed in an ice water bath. Ethanolamine (61 g, 1 mol) and NaOH (40 g, 1 mol) were completely dissolved in water, and then the mixture was added dropwise to the reaction flask over a period of 4 h, as maintaining the temperature of the mixture at 0−5°C.

In the second step, an aqueous solution containing ethylenediamine (30 g, 0.5 mol) and NaOH (40 g, 1.0 mol) was added to the above reaction mixture, which was then heated to 40−60°C. The reaction was allowed to proceed for 4−6 h, maintaining the system at pH < 9.

In the third step, the temperature was increased to 70°C, and the solvent (acetone) was evaporated. A solution of either piperazine (43 g, 0.5 mol) or 1,2-diamino-4-methylcyclopentane (DMCP, 57 g, 0.5 mol) and NaOH (40 g, 1.0 mol) in water was then added to the above reaction mixture, which was heated to reflux. The reaction was allowed to proceed for a given time at a certain temperature, maintaining the system at pH < 10. The mixture was then cooled to room temperature and filtered, and the collected solids were washed and dried, the triazine macromolecules were obtained, CFA1 (yield: 94%) and CFA2 (yield: 91.7%), respectively.

Preparation of IFR-PP composites

Intumescent flame-retardant PP composites (IFR-PP) were prepared by blending PP powder, IFR (containing 76 wt % APP, 19 wt % CFA, and 5 wt % Zeolite 4A), and 1 wt % processing aid (0.7 wt % lubricant EBS and 0.3 wt % antioxidant 1010) by using a high-speed mixer, and then extruded by a twin-screw extruder (D: 20 mm, L/D: 32, model: SLJ-20 Nanjing Jieya Chemical Engineering Equipment Co., China) at a temperature profile of 150°C, 170°C, 185°C, 190°C, 190°C, and 180°C of six heating zones. Testing samples were prepared by injection molding (injector: HTF86X1, Zhejiang Haitian, China) at a temperature profile of 200°C, 210°C, 210°C, and 210°C of four heating zones.

Characterization methods

The structures of the triazine-containing macromolecules were determined by a combination of NMR, FTIR, and elemental analysis. ^{13}C solid-state NMR spectra were recorded on an Infinity-plus 400 spectrometer at 400 MHz. FTIR spectra were recorded from samples pressed into pellets with KBr powder using a Nicolet Avator 360 spectrometer. Elemental analyses were performed with a Carlo Erba 1110 elemental analyzer. The solubilities of the triazine-containing macromolecules were examined by trying to
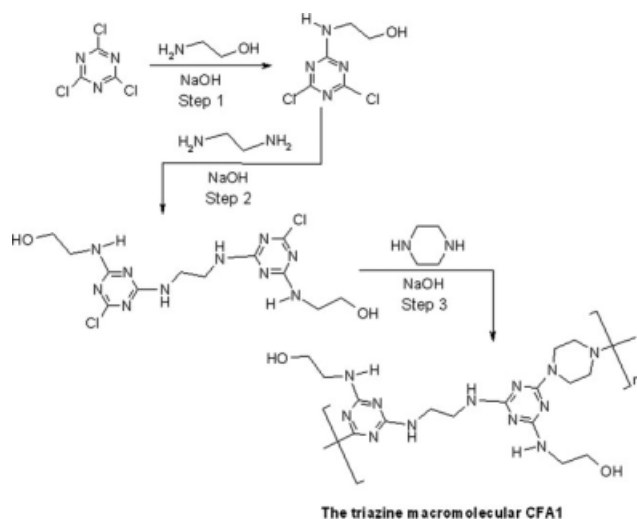
Scheme 1 Synthetic procedure for obtaining the triazine-containing macromolecule CFA1.

dissolve 0.1 g of the respective CFA in 10 mL of solvent. TGA was carried out on a PerkinElmer Pyris 1 thermal analyzer by heating from ambient to 800°C under pure nitrogen at a rate of 10°C min^{-1}, and all samples of TGA data were obtained from a single analysis. The flame retardancy of each sample was evaluated by LOI and UL-94 ratings. The LOI values were measured on a JF-3 oxygen index meter (Jiangning, China) with sheet dimensions of 130 mm × 6.5 mm × 3 mm according to ASTM D2863-97. Vertical burning rates were measured on a CZF-2-type instrument (Jiangning, China) with sheet dimensions of 125 mm × 12.5 mm × 1.6 mm according to the American National Standard UL-94 ASTM D3801. The UL-94 test is commonly used to determine the ignition resistance of materials. The test results are classified by flammability ratings V-0, V-
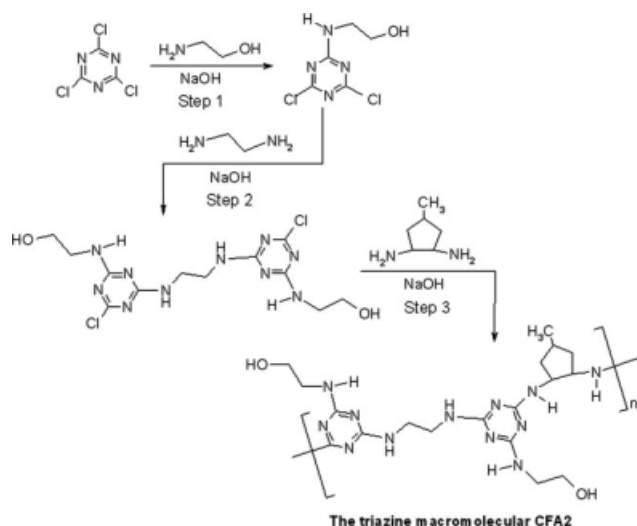
1, or V-2. The V-0 rating indicates a material with the best flame retardancy. The mechanical properties of all samples were performed by Regeer computer controlled mechanical instrument and Notched Izod impact instrument, respectively, according to ASTM standards.

RESULTS AND DISCUSSION

Synthesis and characterization of the triazine-containing macromolecules

The two novel triazine-containing macromolecules, CFA1 and CFA2, which were to serve as both charring agents and foaming agents in IFRs, were synthesized by polycondensation of cyanuric chloride and amine compounds. CFA is used as a general term to mean both CFA1 and CFA2. The polycondensation mechanism is considered as a bimolecular nucleophilic substitution reaction (S_N2) (see Scheme 3).

In the synthetic process, the three active chloride atoms on cyanuric chloride molecule are stepwise replaced (see Schemes 1 and 2); however, they present different reactivity, the first replaced Cl atom on cyanuric chloride molecule is the most active and presents an extraordinarily high reactivity of S_N2, whereas the last replaced Cl atom on cyanuric chloride molecule is the most stable. Therefore, the reaction of Step 1 was carried out at a low temperature (below 5°C), and released a lot of heat, whereas the reaction temperature of Step 2 and Step 3 clearly rises, respectively, the time of the reaction become longer. These results are attributed to the effect of alkyl amino group on electronic cloudy density on the triazine ring after alkylamino group substitutes Cl atom on cyanuric chloride molecule to form C—N bond on the triazine ring. Electronic cloudy density on the triazine ring clearly increases due to strongly donating electronic effect of alkyl amino group, thereby it results in the obvious decrease of the reactivity of Cl atom on the triazine ring. According to data of experimental section, the yield of CFA1 is obviously higher than that of CFA2; this is attributed to the different structures of piperazine and DMCP.

Scheme 2 Synthetic procedure for obtaining the triazine-containing macromolecule CFA2.
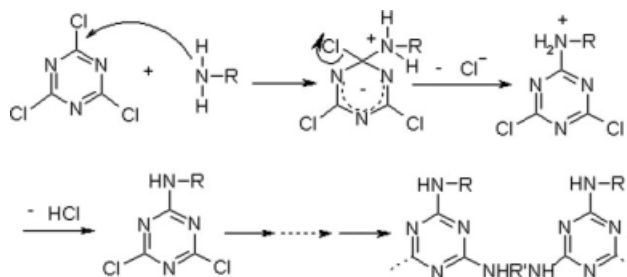
Scheme 3 Mechanism of the polycondensation of cyanuric chloride with alkylamines.
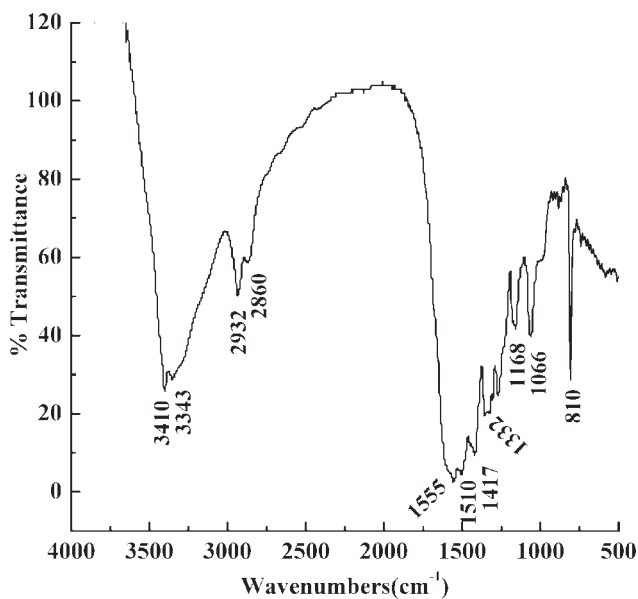
Figure 1 FTIR spectrum of CFA1.

Nitrogen atom on piperazine presents stronger nucleophilic ability that on DMCP, and DMCP shows severer steric hindrance than piperazine.

Figure 1 shows the FTIR spectrum of CFA1. In this spectrum, the broad absorption peaks at 3300–3450 cm^{-1} can be attributed to v_{N-H} and v_{O-H}; the peaks at 2932 cm^{-1} and 2860 cm^{-1} can be assigned to v_{C-H} in $-CH_2-CH_2-$; and those at 1555 cm^{-1}, 1332 cm^{-1}, 1168 cm^{-1}, and 1066 cm^{-1} can be assigned to v_{tr}, v_{tr-N}, v_{C-N}, and v_{C-O}, respectively. The FTIR spectrum of CFA2 is shown in Figure 2. It can be observed that this spectrum is very similar to that of CFA1, with corresponding peaks at 3300–3450 cm^{-1} (v_{N-H} and v_{O-H}), 1513 cm^{-1} (δ_{N-H}), 1410
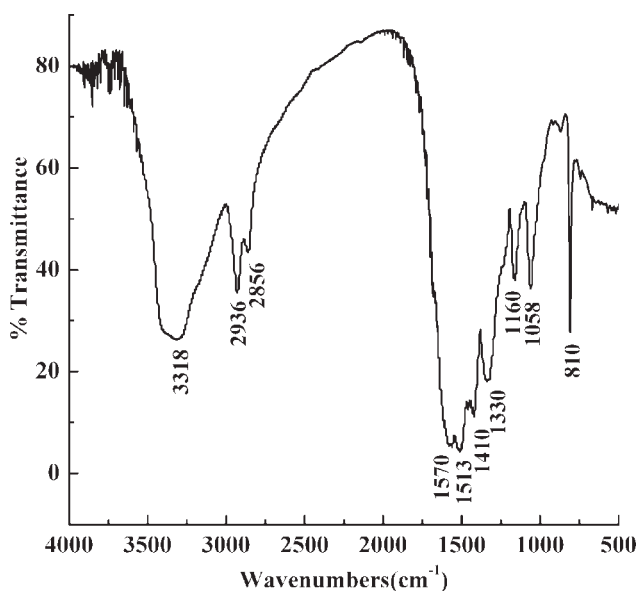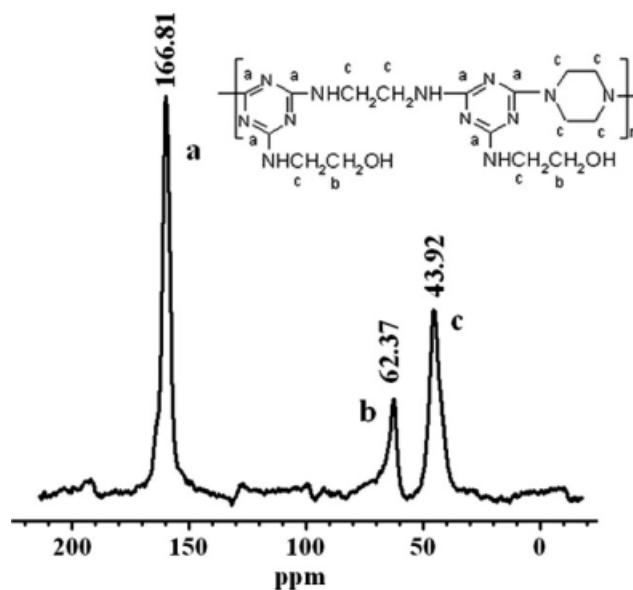

Figure 2 FTIR spectrum of CFA2.

Figure 3 Solid-state ^{13}C-NMR spectrum of CFA1.

cm^{-1} (δ_{O-H}), 810 cm^{-1} (τ_{N-H}); 2936 cm^{-1} and 2856 cm^{-1} (v_{C-H}); 1570 cm^{-1} (v_{tr}), 1332 cm^{-1} (v_{tr-N}), 1160 cm^{-1} (v_{C-N}), and 1058 cm^{-1} (v_{C-O}). The appearance of the characteristic absorption bands of the triazine ring indicates the successful incorporation of this moiety into the synthesized products. Peaks appearing between 3300 cm^{-1} and 3450 cm^{-1} may be assigned to superposition of the v_{N-H} and v_{O-H} bands; but compared with the spectrum of CFA1, one clearly distinct feature of the spectrum of CFA2 is that a wider peak is seen at 3300 cm^{-1} and 3450 cm^{-1}, which may be attributed to the higher content of $-NH-$ in the structure of CFA2. A key characteristic of the FTIR spectra of CFA1 and CFA2 is the disappearance of the peaks 993 cm^{-1}, 838 cm^{-1}, and 534 cm^{-1} attributed to v_{tr-Cl}, which are replaced by the aforementioned peak at 1332 cm^{-1} due to v_{tr-N}.

Figure 3 shows the solid-state ^{13}C-NMR spectrum of CFA1. The respective carbon signals are seen at δ = 43.92 ($\delta_{-NH-CH2-}$), 62.37 (δ_{-CH2OH}), and 166.81 ppm (δ_{tr-C}). Figure 4 displays the solid-state ^{13}C-NMR spectrum of CFA2. It can be seen that the characteristic peak of the triazine ring at δ = 166.81 ppm is also present in this spectrum, along with peaks at δ = 61.70 ppm and 40.99 ppm, which can be assigned to δ_{-CH2OH} and $\delta_{-NH-CH2-}$, respectively. The peak at δ = 37.53 ppm can be ascribed to δ_{-CH2}, δ_{-CH}, and δ_{-CH3}, which is obviously distinct from the signal of CFA1 due to the different structures of CFA2 and CFA1, as shown in Schemes 1 and 2.

Table I lists the elemental analysis data for CFA1 and CFA2. From Table I, it can be seen that the found values were consistent with the calculated values, especially for CFA1, which further confirmed the proposed molecular structures. All of the above
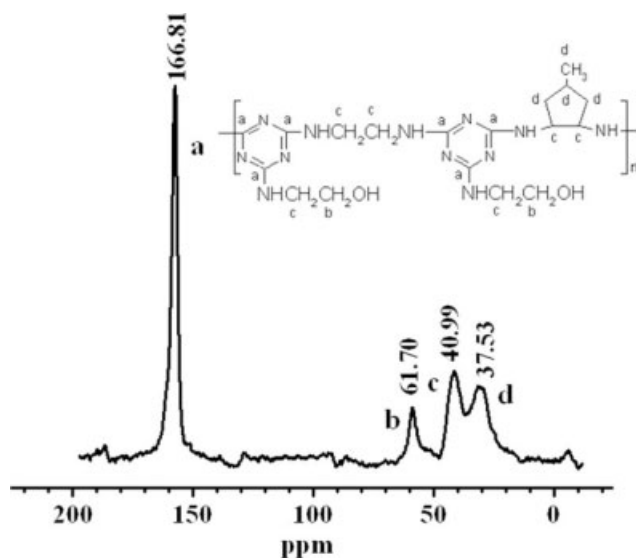
Figure 4 Solid-state ^{13}C-NMR spectrum of CFA2.

facts allowed us to conclude that the polycondensation of cyanuric chloride with amine compounds had successfully yielded the target macromolecules.

Thermal degradation behavior of the CFAs

TGA is the most favored technique for rapid evaluations in comparing and ranking the thermal stability and degradation of various polymers. The TGA data for CFA1 and CFA2 under pure nitrogen are presented in Table II, and the corresponding curves are shown in Figure 5. From Table II and curves a and b in Figure 5, it is evident that CFA1 and CFA2 show high thermal stability. The initial decomposition temperatures of CFA1 and CFA2 were 300.2°C and 287.1°C, respectively, based on 1% mass loss. It can be seen from their TGA curves that they undergo two-step thermal degradation processes. The first thermal degradation step occurs roughly from 290°C to 400°C, it is probably corresponding to chemical reactions of dehydration and release of ammonia, the latter being verified with pH test paper.[26] The second thermal degradation step occurs from about 400°C to 530°C, and may be assigned to decomposition of the macromolecular backbone. The decomposition temperature of CFA1 at second step is much higher than that of CFA2 at second step, the former is 465.5°C and latter is 456.3°C. According to the

TABLE I
Elemental Analysis Data of the Synthesized CFAs

Element sample	Calculated (%)			Found (%)		
	C	N	H	C	N	H
CFA1	45.93	40.19	6.22	45.69	40.11	6.15
CFA2	48.43	37.67	6.73	47.96	36.79	6.79

TABLE II
Thermal Degradation Data for the CFAs Under Pure Nitrogen by TGA

Sample	$T_{initial}$ (°C)	R_{1peak}/T_{1peak} (% min^{-1}/°C)	R_{2peak}/T_{2peak} (% min^{-1}/°C)	Char residue/%	
				600°C	800°C
CFA1	300.2	2.5/336.0	5.7/465.5	48.2	32.2
CFA2	287.1	4.6/331.6	7.0/456.3	30.3	21.1

char residue data in Table II and curves a and b in Figure 5, the char residue of CFA1 was 48.2 wt % at 600°C and 32.2 wt % at 800°C, and that of CFA2 was 30.3 wt % at 600°C and 21.1 wt % at 800°C. The results show that the CFAs display excellent thermal stability and high char residues, which may be attributed to the incorporation of the structurally triazine rings. The fact that CFA1 showed higher thermal stability and charring ability than CFA2 can be attributed to their different macromolecular chain structures. The chain segments of the CFA1
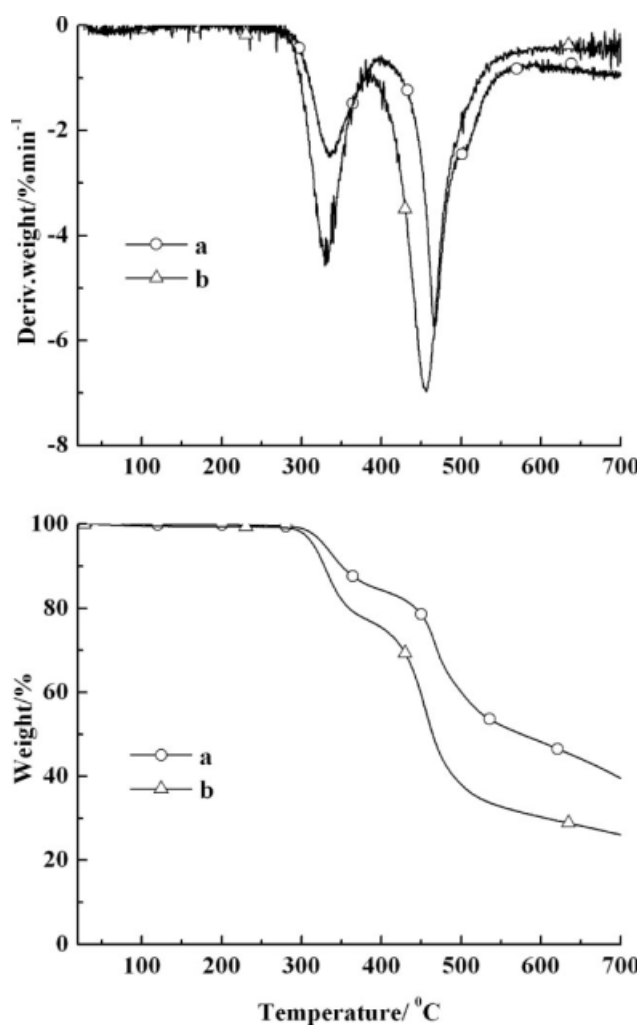

Figure 5 TGA and DTG curves of the CFAs: (a) CFA1 and (b) CFA2.

TABLE III
Influence of the Content of IFR Containing CFA1 on the Flame Retardance of IFR-PP Composites

Sample no.	Composition of IFR-PP (wt %)			Flame retardance	
	PP	IFR	Processing aid	LOI (%)	UL-94
1	99.0	0.0	1.0	17.5	No rating
2	83.0	16.0	1.0	33.5	V-2
3	81.0	18.0	1.0	34.8	V-0
4	79.0	20.0	1.0	36.2	V-0
5	77.0	22.0	1.0	38.2	V-0
6	74.0	25.0	1.0	39.8	V-0

macromolecule incorporate tertiary amino groups and six-membered rings containing tertiary amino groups, whereas there are no tertiary amino groups in the chain segments of the CFA2 macromolecule, as can be seen in Schemes 1 and 2. It has been mentioned that tertiary amino groups present a more important contribution to the thermal stability and charring ability than secondary amino groups.[41,42]

Flame retardant study

As mentioned previously, the introduction of CFA, the structure of which is different from CFA1 and CFA2 synthesized in this article, was expected to enhance the flame retardancy of materials,[39,40] because it could promote the formation of char and increase the extent of foaming during the combustion of composites. LOI values and UL-94 results for the new IFR-PP composites containing CFA1 or CFA2 are presented in Tables III and IV, and Figure 6 shows the photographs of the char formed on the UL-94 bars after testing. From these experimental data, it can be seen that both CFA1 and CFA2, served as new CFAs, showed highly effective flame retardance in the intumescent flame-retardant polypropylene system (IFR-PP). The LOI values of the IFR-PP increased with increasing loading of the IFR. An important feature of the experimental results is that CFA1 imparted superior intumescent flame

TABLE IV
Influence of the Content of IFR Containing CFA2 on the Flame Retardance of IFR-PP Composites

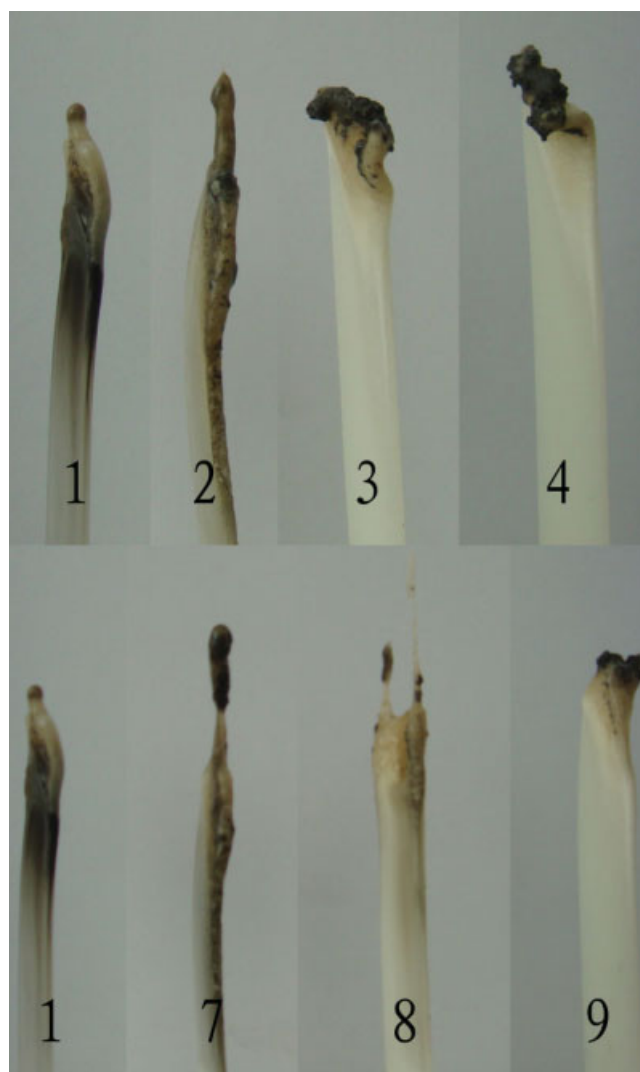| Sample no.	Composition of IFR-PP (wt %)			Flame retardance	
	PP	IFR	Processing aid	LOI (%)	UL-94
1	99.0	0.0	1.0	17.5	No rating
7	83.0	16.0	1.0	30.3	No rating
8	81.0	18.0	1.0	32.1	V-1
9	79.0	20.0	1.0	33.5	V-0
10	77.0	22.0	1.0	35.2	V-0
11	74.0	25.0	1.0	37.2	V-0

Figure 6 Photographs of UL-94 bars with sample number after testing. [Color figure can be viewed in the online issue, which is available at www.interscience.wiley.com.]

retardance compared with CFA2 in the IFR-PP. For instance, when the IFR content was 25 wt %, the LOI value of the IFR-PP containing CFA1 reached 39.8%, whereas that of the IFR-PP containing CFA2 was 37.2%. Besides, when the IFR content was 18 wt %, the LOI value of the IFR-PP containing CFA1 reached 34.8% and the composition could still pass the UL-94 V-0 rating, whereas the LOI value of the IFR-PP containing CFA2 only reached 32.1% and the composition only passed the UL-94 V-1 rating. Their charring behavior shown in Figure 6 further proved this flame retardant result.

Thermal degradation behavior of polypropylene composites

Figures 7 and 8 and Table V give the thermal degradation data and curves of PP, APP, IFR, and IFR-PP system in pure nitrogen. From Figure 1, curve a, the
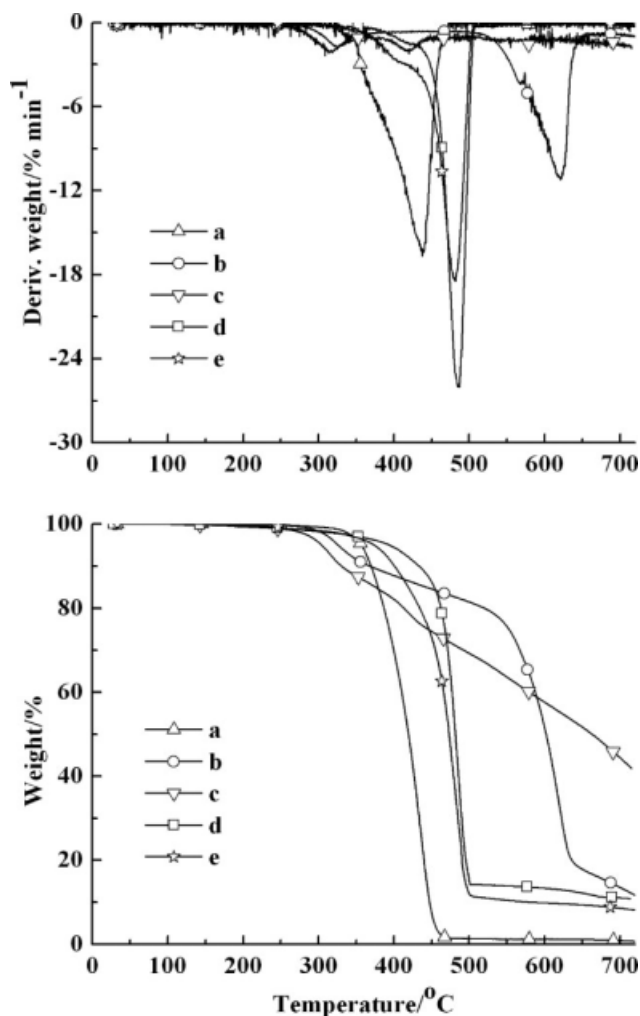
Figure 7 TGA and DTG curves of the APP, PP, IFR1, and IFR1-PP systems: (a) PP, (b) APP, (c) IFR1 containing CFA1, (d) IFR1-PP, and (e) IFR1-PP (calculation).

thermal degradation behavior of PP showed only one peak of PP backbone decomposition at 437.8°C, and the maximum rate of decomposition was very fast (16.7% min^{-1}/°C). There is no char residue remained in PP at over 600°C. The IFR1-PP and IFR2-PP systems have similar TG behavior under the same experimental conditions, having 1% weight loss at 258.2°C and 258.9°C, respectively. However, from the curves d and b in Figures 7 and 8, respectively, we can see that a higher amount of char residue are obtained than PP (Table V), which means that IFR can produce an amount of char residue during thermal degradation process by the reaction of triazine macromolecule containing polyol and APP, like the reaction pentaerithritol and APP.[12]

Based up on curves a, d, in Figure 7 and b in Figure 8, respectively, we found that IFR clearly made a maximum peak of PP decomposition appear at higher temperature. That is, the main decomposition peak of PP took place at 437.8°C, whereas the main decomposition peak of PP in IFR1-PP and

IFR2-PP system appeared at 486.8°C and 484.1°C, respectively. This was because the char layer formed by IFR prevented heat from transferring into inside of IFR-PP materials, and the endothermic reactions took place in IFR charring process, therefore, the thermal stability of IFR-PP was enhanced. Charring ability and thermal degradation behavior further proved that new IFR presents highly flame retardant efficiency in PP system.

According to char residue data in Table V and curves d and e in Figure 7, b and c in Figure 8, respectively, IFR not only changed the thermal degradation behavior of PP but also promoted char formation of PP. The char residue of IFR1 and IFR1-PP is much higher than that of IFR2 and IFR2-PP, respectively. This fact demonstrated that the CFA1 presents much more charring ability than CFA2. It is attributed to their differently chemical structure that CFA1 contains tertiary amino groups and six-membered rings, whereas CFA2 contains no tertiary amino groups. The previous researches have been
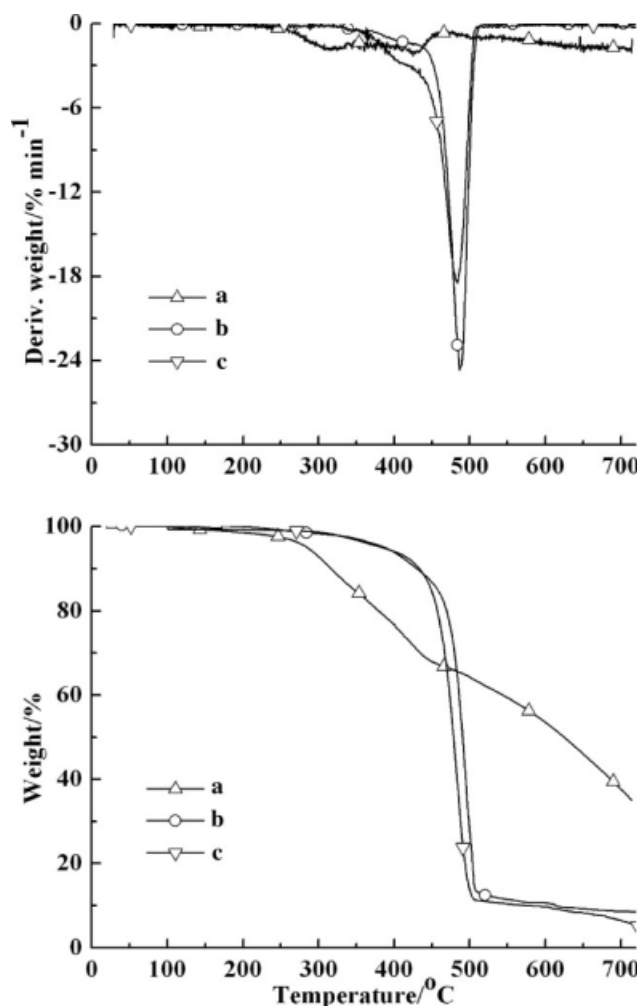

Figure 8 TGA and DTG curves of the IFR2 and IFR2-PP systems: (a) IFR2 containing CFA2, (b) IFR2-PP, and (c) IFR2-PP (calculation).

TABLE V
Thermal Degradation and Char Residue Data of APP, PP, IFR, and IFR-PP Systems Obtained by TGA

Sample	$T_{initial}$ (°C)	R_{1peak}/T_{1peak} (% min^{-1}/°C)	R_{2peak}/T_{2peak} (% min^{-1}/°C)	R_{3peak}/T_{3peak} (% min^{-1}/°C)	Char residue/% 600°C	700°C
PP	320.2	16.7/437.8	–	–	1.2	0
APP	288.5	1.7/324.0	11.1/622.3	–	51.4	13.5
IFR1 (with CFA1)	242.7	2.1/318.9	2.2/421.2	1.6/578.9	57.6	44.5
IFR1-PP	258.2	26.0/486.7	–	–	13.4	11.1
IFR1-PP (calculation)	257.8	18.5/481.1			9.9	8.6
IFR2 (with CFA2)	215.7	1.9/324.2	2.3/424.7	1.4/561.0	52.3	37.6
IFR2-PP	258.9	24.5/484.4.3	–	–	10.7	8.7
IFR2-PP (calculation)	266.5.5	18.3/481.7	–	–	9.8	6.5

proved that nitrogen compounds containing tertiary amino group are more beneficial to char formation and thermal stability than that containing no tertiary amino group.[41,42]

Mechanical properties

Tables VI and VII give the data of the mechanical properties of IFR-PP systems. IFR components were kept consistent in IFR-PP, that is, 19 wt % CFA, 76% APP, 5 wt % 4A zeolite. In general, IFRs showed a little effect on the mechanical properties of IFR-PP.

When compared with pure PP based on Tables VI and VII, IFR1 and IFR2 clearly enhanced Notched Izod Impact strength, which was increased from 2.8 to about 4 kJ m^{-2}, whereas the loading of IFR only gave little effect on Notched Izod Impact strength; however, the tendency is different. Both IFR1 (CFA1) and IFR2 (CFA2), the high loading of IFR2 seemingly was beneficial to Notched Izod Impact strength. Tensile strength of IFR-PP gradually decreased with the increase of IFR loading. IFR2 presented less effect on tensile strength of IFR-PP than IFR1, for instance, when the loading of IFR is 25 wt % in IFR-PP system, tensile strength of IFR1-PP is 27.4 MPa, whereas 28.7 MPa for IFR2-PP. According to data of the flexural strength, IFR2 enhanced the flexural strength of IFR2-PP. From the analysis of mechanical properties of IFR-PP, IFR2 shows more advantageous effect on mechanical properties of IFR-PP than IFR1. This is because they contain dif-

ferent CFAs, IFR1 with CFA1 and IFR2 with CFA2. Based on their different chemical chain structures (Schemes 1 and 2), the macromolecular chain of CFA2 contains methyl groups, which probably increase the compatibility of PP and CFA2 (IFR2).

CONCLUSIONS

Two novel triazine-containing macromolecules with polyol groups (CFA1 and CFA2) have been successfully synthesized and their chemical structures have been confirmed by FTIR, ^{13}C solid-state NMR, and elemental analysis. TGA tests have indicated that CFA1 and CFA2 show high thermal stability and very high propensity for char formation, with CFA1 presents a higher charring ability than CFA2. These results are attributed to the presence of tertiary amino groups and six-membered rings containing tertiary amino groups within the macromolecular chain of CFA1, whereas CFA2 lacks these structural features. Based on experimental results of LOI and UL-94 rating of IFR-PP, CFA1 has been found to display more effective flame retardance than CFA2, the LOI value of FR-PP reaching 34.8 and the composition passing the UL-94 V-0 rating (1.6 mm), when the IFR1 content was only 18 wt %. The TGA curves of APP, PP, IFR, and IFR-PP showed that IFR could change the thermal degradation behavior of PP, and promote PP to form char, based upon the results of the calculation and the experiment. It has been

TABLE VI
Mechanical Properties of PP-IFR Composites with Different Loadings of IFR1

Sample no.	Composition of IFR1-PP (wt %) PP	IFR1	Processing aid	Mechanical properties Tensile strength (MPa)	Flexual strength (MPa)	Izod impact strength (kJ m^{-2})
1	99.0	0	1.0	32.8	38.1	2.8
2	83.0	16	1.0	29.7	38.2	4.2
3	81.0	18	1.0	29.4	38.2	4.2
4	79.0	20	1.0	29.2	38.4	4.1
5	77.0	22	1.0	28.6	38.4	4.0
6	74.0	25	1.0	27.4	38.5	3.9

TABLE VII
Mechanical Properties of PP-IFR Composites with Different Loadings of IFR2

Sample no.	Composition of IFR2-PP (wt %)			Mechanical properties		
	PP	IFR2	Processing aid	Tensile strength (MPa)	Flexual strength (MPa)	Izod impact strength (kJ m^{-2})
1	99.0	0	1.0	32.8	38.1	2.8
7	83.0	16	1.0	30.5	41.0	4.0
8	81.0	18	1.0	30.0	41.2	4.0
9	79.0	20	1.0	29.2	41.8	4.0
10	77.0	22	1.0	28.9	41.7	4.3
11	74.0	25	1.0	28.7	41.7	4.4

further confirmed that the charring ability and flame retardancy of triazine-containing macromolecules are influenced by the structure of the macromolecular chain. From the result of mechanical properties tests, IFR-PP composites adding IFRs with CFA1 and CFA2 showed good mechanical properties.

References

1. Green, J. In Flame Retardant Polymeric Materials;Lewin, M., Atlas, S. M., Pearce, E. M., Eds.; Plenum Press: New York, 1982; Vol. 3.
2. Inata, H.; Maki, I.; Ishikawa, T.; Takeda, K. J Appl Polym Sci 2006, 99, 2152.
3. Ma, H. Y.; Tong, L. F.; Xu, Z. B.; Fang, Z. P.; Jin, Y. M.; Lu, F. Z. Polym Degrad Stab 2007, 92, 720.
4. Utracki, L. A.; Sepehr, M.; Boccaleri, E. Polym Adv Technol 2007, 18, 1.
5. Zhang, Y.; Hu, Y.; Song, L.; Wu, J.; Fang, S. Polym Adv Technol 2008, 19, 960.
6. Marosfoi, B. B.; Garas, S.; Bodzay, B.; Zubonyai, F.; Marosi, G. Polym Adv Technol 2008, 19, 693.
7. Liu, Y.; Wang, D. Y.; Wang, J. S.; Song, Y. P.; Wang, Y. Z. Polym Adv Technol 2008, 19, 1566.
8. Jang, B. N.; Jung, I; Choi, J. J Appl Polym Sci 2009, 112, 2669.
9. Zhou, S.; Wang, Z. Z.; Gui, Z.; Hu, Y. J Appl Polym Sci 2008, 110, 3804.
10. Hoang, D. Q.; Kim, J.; Jang, B. N. Polym Degrad Stab 2008, 93, 2042.
11. Lu, S. Y.; Hamerton, I. Prog Polym Sci 2002, 27, 1661.
12. Camino, G.; Costa, L.; Martinasso, G. Polym Degrad Stab 1989, 23, 359.
13. Le Bras, M.; Bugajny, M.; Lefebvre, J.; Bourbigot, S. Polym Int 2000, 49, 1115.
14. Xie, F.; Wang, Y. Z.; Yang, B.; Liu, Y. Macromol Mater Eng 2006, 291, 247.
15. Heibrich, H.; Stefan, P. Polym Int 2000, 49, 1106.
16. Huang, Z. G.; Shi, W. F. Eur Polym J 2007, 43, 1302.
17. Ikuta, N.; Suzuki, Y.; Maekawa, Z.; Hamada, H. Polymer 1993, 34, 2445.
18. Li, L. P.; Li, B.; Tang, F. Eur Polym J 2007, 43, 2604.
19. Ravadits, I.; Tóth, A.; Marosi, G.; Márton, G.; Szép, A. Polym Degrad Stab 2001, 74, 419.
20. Huang, H. H.; Tian, M.; Liu, L.; He, Z. H.; Chen, Z. Q.; Zhang, L. Q. J Appl Polym Sci 2006, 99, 3203.
21. Baljinder, K. K.; Horrocks, A. R. Polym Degrad Stab 1996, 54, 289.
22. Sabyasachi, G.; Gang, S.; Katherine, H.; Mark, H. E. Polym Degrad Stab 2008, 93, 99.
23. Horacek, H.; Grabner, R. Polym Degrad Stab 1996, 54, 205.
24. Chiu, S. H.; Wang, W. K. Polymer 1998, 39, 1951.
25. Camino, G.; Costa, L.; Martinasso, G. Polym Degrad Stab 1990, 28, 17.
26. Bourbigot, S.; Le Bras, M.; Duquesne, S.; Rochery, M. Macromol Mater Eng 2004, 289, 499.
27. Seymour, R. B.; Kirshenbaum, G. S. High Performance Polymers: Their Origin and Development; Elsevier: New York, 1986. p 309.
28. Nishikubo, T.; Kameyama, A.; Saito, C. J Polym Sci Part A: Polym Chem 2000, 38, 3604.
29. Saito, Y.; Kamio, K.; Shiomi, H. Jpn. Pat. 63,273,644 (1988).
30. Takei, M.; Washimi, A.; Yoshida, M.; Kimura, K. Jpn. Pat. 04,330,066 (1992).
31. Saida, K.; Sakai, M.; Narahara, T. Jpn. Pat. 52,136,298 (1977).
32. Hu, X. P.; Li, W. Y.; Wang, Y. Z. Appl Polym Sci 2004, 94, 1556.
33. Narita, N.; Otsutomocho, K. Eur. Pat. 058,306,5A1 (1994).
34. Peter, H.; Peter, K. H.; Ammann, J.; Andre, P. U.S. Pat. 3,149,100 (1964).
35. Cipolli, R.; Criani, R.; Nucida, G. Eur. Pat. 448,774 (1992).
36. Hu, X. P.; Li, W. Y.; Wang, Y. Z. Macromol Mater Eng 2004, 289, 208.
37. Li, B.; Jia, H.; Guan, L. M.; Bing, B. C.; Dai, J. F. J Appl Polym Sci 2009, 114, 3626.
38. Wang, H. F.; Li, B. Polym Adv Technol, to appear.
39. Li, B.; Xu, M. J. Polym Degrad Stab 2006, 91, 1380.
40. Li, Y. T.; Li, B.; Dai, J. F. Polym Degrad Stab 2008, 93, 9.
41. Boyer, C.; Boutevin, G.; Robin, J. J.; Boutevin, B. Polymer 2004, 45, 7863.
42. Cervantes-Uc, J. M.; Cauich-Rodríguez, J. V.; Herrera-Kao, W. A.; Vázquez-Torres, H.; Marcos-Fernández, A. Polym Degrad Stab 2008, 93, 1891.